Geometric properties of two-dimensional O(*n*) loop configurations

2007 J. Phys. A: Math. Theor. 40 3305

(http://iopscience.iop.org/1751-8121/40/13/001)

J. Phys. A: Math. Theor. **40** (2007) 3305–3317 doi:10.1088/1751-8113/40/13/001

Geometric properties of two-dimensional O(n) loop configurations

Chengxiang Ding[1], Youjin Deng[2], Wenan Guo[1], Xiaofeng Qian[3] and Henk W J Blöte[3,4]

[1] Physics Department, Beijing Normal University, Beijing 100875, People's Republic of China
[2] Department of Physics, New York University, 4 Washington Place, New York, NY 10003, USA
[3] Instituut Lorentz, Universiteit Leiden, Postbus 9506, 2300 RA Leiden, The Netherlands
[4] Faculty of Applied Sciences, Delft University of Technology, PO Box 5046, 2600 GA Delft, The Netherlands

Received 28 November 2006, in final form 7 February 2007
Published 14 March 2007
Online at stacks.iop.org/JPhysA/40/3305

Abstract
We study the fractal geometry of O(n) loop configurations in two dimensions by means of scaling and a Monte Carlo method, and compare the results with predictions based on the Coulomb gas technique. The Monte Carlo algorithm is applicable to models with noninteger n and uses local updates. Although these updates typically lead to nonlocal modifications of loop connectivities, the number of operations required per update is only of order 1. The Monte Carlo algorithm is applied to the honeycomb O(n) model for several values of n, including noninteger ones. We thus determine scaling exponents that describe the fractal nature of O(n) loops at criticality. The results of the numerical analysis agree with the theoretical predictions.

PACS numbers: 64.60.Ak, 64.60.Fr, 64.60.Kw, 75.10.Hk

1. Introduction

The O(n) model [1] consists of n-component spins $\vec{s}_i = \left(s_i^1, s_i^2, \ldots, s_i^n\right)$ on a lattice, with isotropic, i.e., O(n) invariant couplings. The common form of the reduced Hamiltonian of the O(n) spin model is

$$H = -\frac{J}{k_{\mathrm{B}}T} \sum_{\langle i,j \rangle} \vec{s}_i \cdot \vec{s}_j, \tag{1}$$

where the indices i and j represent lattice sites, and the sum is over all nearest neighbour pairs, J is the coupling constant, k_{B} is Boltzmann's constant and T is the temperature. Thus, the partition function of the model is

$$Z_{\mathrm{spin}} = \int \prod_{\langle i,j \rangle} \exp\left(\frac{J}{k_B T} \vec{s}_i \cdot \vec{s}_j\right) \prod_k \mathrm{d}\vec{s}_k, \tag{2}$$

where the spins are normalized such that $\vec{s}_k \cdot \vec{s}_k = n$. This model includes as special cases the Ising, the XY and the Heisenberg model, for $n = 1$, 2 and 3, respectively.

In the high-temperature limit, the bond weight $w(\vec{s}_i \cdot \vec{s}_j)$ reduces in first order to $(1 + x\vec{s}_i \cdot \vec{s}_j)$, with $x = J/(k_B T)$. Thus, in this limit, the partition function of the model (1) takes the form

$$Z_{\text{spin}} = \int \prod_{\langle i,j \rangle} (1 + x\vec{s}_i \cdot \vec{s}_j) \prod_k \mathrm{d}\vec{s}_k. \tag{3}$$

This expression still satisfies the O(n) symmetry implied by equation (1). Apart from a high-T approximation for model (1), equation (3) can be interpreted as the exact partition integral of an O(n) symmetric model with reduced pair potential $-\ln(1 + x\vec{s}_i \cdot \vec{s}_j)$.

According to the universality hypothesis, the universality class of a phase transition is determined by only very few parameters including the dimensionality of the model, and the range and the symmetry of the spin–spin interactions. It is thus reasonable to expect [2] that the reduced Hamiltonian that corresponds with equation (3), namely $H = -\sum_{\langle i,j \rangle} \ln(1 + x\vec{s}_i \cdot \vec{s}_j)$ with $x = J/(k_B T)$ not necessarily small, still belongs to that of equation (1), i.e., the O(n) universality class in two dimensions. Indeed the results for the model (3) for $n = 2$ appear to agree with the theory of Kosterlitz and Thouless [3] for the XY model. One may note here that first-order transitions are possible in models with O(2) symmetry [4], but only in the case of rather extreme deviations from equation (1).

The O(n) model (3) on the honeycomb lattice can be mapped onto the O(n) loop model [5] on the same lattice, with a partition sum

$$Z_{\text{loop}} = \sum_G x^{N_b} n^{N_l}, \tag{4}$$

where the graph G covers N_b bonds of the lattice, and consists of N_l closed, non-intersecting loops. The sum is on all such graphs. In the language of the O(n) loop model, x is the weight of a bond visited by a loop, and n is the loop weight. The exact equivalence shows that equation (4) belongs to the same universality class as equation (3). Note however that n is no longer restricted to be an integer in equation (4).

The research of O(n) models is a subject of a considerable history, in which a prominent place is occupied by the exact results [2] for the O(n) loop model on the honeycomb lattice. These results include the critical points for $-2 \leqslant n \leqslant 2$, and the temperature and the magnetic exponent.

Also the geometric description of fluctuations at and near criticality has a long history, which goes back to the formulation of phase transitions in terms of the droplet model [6]. For the q-state Potts model (for a review, see [7]), it was found that the fractal dimension of Kasteleyn–Fortuin (KF) clusters [8] is equal to the magnetic scaling exponent y_h. More generally, geometric Potts clusters can be defined by connecting neighbouring, equal Potts spins by a bond percolation process. Several new critical exponents were found by Coulomb gas and other methods [9–12]. These exponents describe the geometric properties and the renormalization flow of this model.

The fractal dimension d_l of loops in the critical O(n) loop gas can be obtained in various ways. Without direct reference to the Coulomb gas, it is still possible to obtain a clue from the relation [12, 13] between the exponents describing random clusters of the tricritical Potts model, and those describing Potts clusters in the critical Potts model. From the equivalence of the critical O(n) model and the tricritical $q = n^2$-state Potts model [2], one can thus associate the fractal dimension d_l of the critical O(n) loop gas with the hull fractal dimension of critical Potts clusters. The latter dimension was conjectured by Vanderzande [14]. However, the

known correspondence of the O(n) model with the Coulomb gas [15] provides the same result for d_l in a more direct way.

In the present paper, we focus on d_l as the fundamental non-thermodynamic scaling dimension behind some geometric properties of O(n) loop configurations. We relate d_l to some exponents describing such properties. These exponents are exact.

While theoretical predictions are available, thus far there is no numerical evidence in support of these, except for the Ising case $n = 1$ or $q = 2$ [13]. One of the reasons behind this situation may be that the Boltzmann weights in the O(n) partition sum depend, at least for $n \neq 1$, on the number of loops. The nonlocal character of these loops renders the O(n) loop models somewhat difficult to handle by Monte Carlo simulations. Nevertheless, such algorithms have been constructed [18, 19]. One may propose a local Monte Carlo move and construct a valid acceptance probability from the condition of detailed balance, while taking into account the change of the number of loops and their total length due to this move. While the determination of the change of length is a local task, the determination of the change of the number of loops is not, and for a critical O(n) model it requires a number of operations that increase algebraically with the system size L. Critical slowing down can make this situation even worse, so that this way of simulation is restricted to rather small system sizes.

Until now, a sufficiently efficient Monte Carlo algorithm for the O(n) loop model has not been described. Therefore, in this work, we develop a new Monte Carlo algorithm, which is applicable to models with noninteger $n > 1$ and uses local updates. Although these updates typically lead to nonlocal modifications of the loop connectivities, the number of operations required per update is only of order 1, and essentially independent of the system size.

We then apply the algorithm to the critical O(n) loop model and determine exponents of some geometric observables. The results agree with the theoretical predictions.

The outline of the rest of this paper is as follows. In section 2 we show how a fundamental non-thermodynamic scaling dimension behind some geometric properties of O(n) loops can be derived exactly from a mapping onto the Coulomb gas, and how it relates to exponents describing some geometric observables. Section 3 introduces the Monte Carlo algorithm. In section 4 we apply the algorithm to the critical O(n) loop model and determine exponents of some geometric observables.

2. Coulomb gas derivation and scaling formulae

It is well known that geometric and fractal properties of O(n) loops and various types of critical clusters can be analysed by means of a mapping onto the Coulomb gas [15, 20]. A number of exact scaling dimensions were obtained by this technique, see e.g., [11, 15–17, 21]. Here we base ourselves on these analyses, which rely on a reformulation of correlation functions $g(r)$ in the model of interest in terms of the Coulomb gas. The dimensions $X(e, m)$ associated with such correlation functions are described by pairs of electric and magnetic charges, (e_0, e_r) and (m_0, m_r), separated by a distance r:

$$X(e, m) = -\frac{e_0 e_r}{2g} - \frac{m_0 m_r g}{2}, \tag{5}$$

where g is the coupling constant of the Coulomb gas. For the critical O(n) model it is given by

$$g = 1 + \frac{1}{\pi}\arccos\frac{n}{2}, \tag{6}$$

where we use a normalization that is in agreement with a part of the earlier literature, but different from that used in [15] (our g is four times smaller, and the charges differ by a factor 2 such that the $X(e, m)$ are the same).

Let us now consider the correlation function at criticality describing the probability that two lattice edges separated by a distance r are parts of the same loop. It decays with an exponent $2X_l$, where X_l is the O(n) loop scaling dimension. The exponent X_l is described by a pair of magnetic charges $m_0 = -m_r = 1$ and a pair of electric charges $e_0 = e_r = 1 - g$. This leads to

$$X_l = 1 - \frac{1}{2g}. \tag{7}$$

This dimension X_l is the renormalization exponent behind geometrical and fractal properties of O(n) loops, just as the renormalization exponents X_t and X_h determine the thermodynamic singularities. The dimension X_l is equivalent with the hull exponent of percolation clusters [16], which involves the same magnetic and electric charges as a function of g.

In another application of the Coulomb gas technique we can explore corrections to scaling associated [11] with the exponent X_{2l} that describes the decay of the probability that two O(n) loops collide in two points separated by a distance r. The value of this exponent is determined by electric charges as above and magnetic charges $m_0 = -m_r = 2$:

$$X_{2l} = 1 - \frac{1}{2g} + \frac{3g}{2}. \tag{8}$$

This exponent becomes marginal at $n = 2$ and is thus expected to lead to poor convergence of finite-size data near $n = 2$.

The physical relevance of X_l can be demonstrated by means of scaling arguments. The probability $g_l(r)$ that two points at a distance r lie on the same loop is, as given above, $g_l(r) \simeq ar^{-2X_l}$. Let, at criticality, the fractal dimension of the loops be d_l. Thus, under a rescaling by a factor b, the length l of the loop decreases by a factor b^{d_l}, and its density increases by a factor b^{2-d_l}. This determines the correlation in the rescaled system as $g_l(r/b) \simeq ab^{4-2d_l}r^{-2X_l}$ which is, as specified above, to be compared with $g_l(r/b) \simeq ab^{2X_l}r^{-2X_l}$. It thus follows that the fractal dimension of loops is

$$d_l = 2 - X_l. \tag{9}$$

Let $P_l(l)$ be the density of loops of length l. It is natural that, at criticality, $P_l(l)$ depends algebraically on l, with an exponent denoted as p_l:

$$P_l(l) \propto l^{p_l}. \tag{10}$$

Under a rescaling by a linear factor b, the loop density is affected for two reasons: first, the loops decrease in length by a factor $b^{d_l} = b^{2-X_l}$, and second, the density increases by a factor b^2 because the volume is reduced. Consistency requires that $P_l(l)\,\mathrm{d}l = b^{-2}P_l(lb^{2-X_l})\,\mathrm{d}(lb^{2-X_l})$ or $P_l(l) = b^{-X_l}P_l(lb^{2-X_l})$. The requirement $P_l(l) \propto l^{-p_l}$ yields $l^{-p_l} = (lb^{-2+X_l})^{-p_l}b^{-2+X_l-2}$. Matching the exponents shows that

$$p_l = 1 + \frac{2}{2 - X_l}. \tag{11}$$

The linear size of the largest loops (the diameter of the box where they fit in) is naturally associated with the correlation length. Thus, scaling implies that the divergence of the expectation value of the linear size of the largest loop goes as $(x_c - x)^{-\nu} = (x_c - x)^{-1/y_t}$ when the critical point is approached, and the actual length $l_{\max}(x)$, as expressed in lattice edges, behaves as a power $2 - X_l$ of the linear size, it follows that the largest loop length diverges as

$$l_{\max}(x) \propto (x_c - x)^{(X_l-2)/y_t}. \tag{12}$$

For $L \to \infty$ and $x > x_c$, there exists an infinite spanning loop. Under a rescaling by a linear scale factor b its density increases by a factor b^{X_l} while, as usual, the temperature field

$t \propto x - x_c$ scales as $t \to t' = b^{y_t} t$. The fraction $s_l(x - x_c)$ of the edges covered by the spanning loop scales as $s_l(b^{y_t}(x_c - x)) = b^{X_l} s_l(x_c - x)$. The choice $b = (x_c - x)^{-1/y_t}$ leads to a constant on the left-hand side of this equation, and after substitution on the right-hand side, the scaling behaviour follows as

$$s_l(x_c - x) \propto (x_c - x)^{X_l/y_t}. \tag{13}$$

The finite-size dependence of the similar fraction $s_l(L)$ of a system with the finite size L at criticality, which is the fraction of the edges covered by the largest loop, can simply be found by rescaling the system to a given size, say 1. This leads to

$$s_l(L) \propto L^{-X_l}. \tag{14}$$

Including a correction to scaling, we may modify this into

$$s_l(L) = aL^{-X_l}(1 + bL^{y_i} + \cdots), \tag{15}$$

where $y_i = 2 - X_{2l}$ is a candidate for the leading correction exponent [11] and a and b are unknown amplitudes.

In analogy with magnetic systems, a susceptibility-like quantity χ_l can be defined on the basis of the distribution of the loop sizes as

$$\chi_l \equiv \sum_{l=1}^{l_{\max}} P_l(l) l^2. \tag{16}$$

According to the aforementioned scaling behaviour, the largest loop in a critical system of finite size L has a length scale $l_{\max} \propto L^{2-X_l}$. Thus

$$\chi_l(L) \propto \sum_{l=1}^{L^{2-X_l}} l^{2-p_l}. \tag{17}$$

Substitution of $p_l = 1 + 2/(2 - X_l)$ yields

$$\chi_l(L) \propto L^{2-2X_l}. \tag{18}$$

Again, we can include corrections to scaling

$$\chi_l(L) = cL^{2-2X_l}(1 + \mathrm{d}L^{y_i} + \cdots), \tag{19}$$

with y_i as mentioned above, and c and d are unknown constants.

Another correlation function of interest describes the probability that two sites on the dual triangular lattice separated by a distance r sit inside the same loop (i.e., not separated by any loop of the model). The exponent X_a describing the decay of this function at criticality was derived by Duplantier and Saleur [17] as $X_a = 1 - g/2 - 3/(8g)$. The fractal dimension of the interior of O(n) loops is therefore $d_a = 2 - X_a = 1 + g/2 + 3/(8g)$. The area inside a loop does not include the area inside loops enclosed by that loop. The exponent X_a thus also determines the finite-size scaling of the spanning loop. We are therefore interested in the fraction s_a of the dual lattice sites that sit inside the largest loop. Scaling indicates that this quantity is subject to the following finite-size behaviour:

$$s_a(L) \propto L^{-X_a}. \tag{20}$$

We furthermore define another susceptibility-like quantity χ_a on the basis of the distribution $P_a(a)$ of the area a (expressed in the number of enclosed sites of the dual lattice) of the interior of the loops as

$$\chi_a(L) \equiv \sum_a P_a(a) a^2, \tag{21}$$

which is expected to scale as

$$\chi_a(L) \propto L^{2-2X_a}. \tag{22}$$

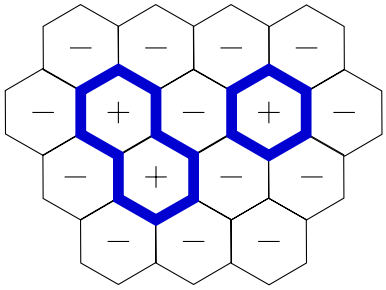

Figure 1. Representation of a loop configuration with Ising spins.

3. Monte Carlo algorithm

In the existing Monte Carlo algorithm for the loop model the local updates require time-consuming nonlocal operations as explained above, somewhat analogous to the nonlocal operations described by Sweeny for the Monte Carlo simulation of the random-cluster model [22]. To get rid of these nonlocal operations we adopt the following procedure.

As a first step of such an algorithm for the simulation of the O(n) loop model on the honeycomb lattice, we represent the loop configuration by means of Ising spins on the dual lattice, which is triangular. The loops are just the interfaces between neighbouring spins of a different sign. We restrict ourselves to systems with periodic boundary conditions, so that the interfaces indeed form a system of closed, nonintersecting loops on the honeycomb lattice. This is illustrated in figure 1 using a loop configuration which consists of 2 loops and 16 bonds, shown as bold lines. This graph contributes a weight $x^{16}n^2$ to the partition function. The loops can of course be represented by two opposite Ising spin configuration, but this degeneracy has no further consequences for our line of argument.

We now show how one can update the loop configuration by means of local Metropolis-type updates of the dual Ising spins representing the loop configuration. It works only for $n \geqslant 1$. The essential element of this approach is that, given a loop decomposition, colour variables (for instance, binary variables) are assigned to the loops. The weights of the colours add up to n. Summation on the colour variables thus reproduces the O(n) partition sum. One of the weights is chosen equal to 1, so that any change of the number of loops of the corresponding colour does not change the weight associated with those loops. Thus the transition probabilities of a Monte Carlo move that does not affect the loops of the other colour depend only on the change of the number of edges covered by the loop configuration. Since each loop segment corresponds with a pair of antiparallel dual spins, the bond weight x simply relates to the Ising coupling K.

One unit of importance sampling is realized by the following operations, which are to be repeated cyclically:

(i) For each loop, assign its colour to be either 'green' with probability $1/n$ or 'red' with the remaining probability $1 - 1/n$.
(ii) Randomly select an Ising spin on the dual lattice.
(iii) Check if the spin is adjacent to a red loop segment. If so, do nothing; if not, update the spin using the Metropolis probabilities, with Ising couplings K determined as $\mathrm{e}^{-2K} = x$.
(iv) Repeat steps (ii) and (iii) until the number of update attempts is equal to the number of sites of the dual lattice.
(v) Perform a sweep through the Ising system to find all loops.

Table 1. Numerical data for $s_l(L)$, $\chi_l(L)$ and $s_a(L)$, $\chi_a(L)$ for different system sizes L at the critical point of the O($n = 1.5$) model.

L	s_l		χ_l		s_a		χ_a	
8	0.129 07	(2)	0.8648	(1)	0.810 28	(3)	2.166	(1)
16	0.086 11	(2)	2.1984	(3)	0.763 86	(5)	8.439	(6)
24	0.067 85	(3)	3.4141	(6)	0.738 29	(8)	18.39	(2)
32	0.057 18	(3)	4.5578	(8)	0.721 08	(9)	31.66	(5)
40	0.050 06	(4)	5.6466	(11)	0.708 12	(11)	48.15	(9)
48	0.045 04	(4)	6.6993	(14)	0.697 29	(13)	68.11	(14)
56	0.041 07	(4)	7.7199	(23)	0.688 69	(16)	90.80	(24)
64	0.037 93	(4)	8.7142	(25)	0.681 30	(15)	116.3	(3)
80	0.033 24	(4)	10.635	(3)	0.668 99	(19)	176.6	(6)
96	0.029 87	(4)	12.477	(6)	0.658 95	(22)	249.0	(10)
112	0.027 23	(5)	14.273	(6)	0.650 95	(26)	330.7	(14)
128	0.025 13	(5)	16.027	(8)	0.6441	(3)	422.4	(23)

(vi) Repeat steps (i)–(v) a fixed number $n_s - 1$ times.
(vii) Sample the data of interest from the loop configuration.

A Monte Carlo run consists of many of these cycles, each of which thus includes n_s Metropolis-like sweeps, new random assignments of loop colours and the data sampling procedure. In spite of the nonlocal nature of the O(n) loop model, the number of operations per cycle with n_s Metropolis-like sweeps is of order $n_s L^2$, just as for local updates for models with *local* interactions. The introduction of loop colours preserves their total weight, and the Ising flips, which are the only steps that change the loop configuration, satisfy the conditions of detailed balance. Therefore, the algorithm should indeed generate configurations in accordance with Boltzmann statistics. Tests confirm that the simulation results agree with those of the existing algorithm [19]. Since this algorithm assigns colours to the loops, we refer to it as 'colouring algorithm'.

4. Simulation

With the help of the algorithm described above, we simulated the O(n) model on the honeycomb lattice at the exactly known [2] critical points $x_c = (2 + (2 - n)^{1/2})^{-1/2}$ in order to check the theoretical predictions described in section 2.

We first applied our algorithm to the case $n = 1.5$, using 12 system sizes in the range $8 \leqslant L \leqslant 128$, where L is the linear size of the dual triangular lattice, and periodic boundary conditions. For each system size, a run was executed with a length of 4×10^7 Monte Carlo cycles after equilibration of the system. Each cycle included $n_s = 5$ sweeps and loop formation steps, and one sampling as described above. Statistical errors were estimated by means of binning in 2000 partial results.

The data sampling included the density $P_l(l)$ of loops of length l. The results for the system of size $L = 128$ are shown in figure 2. It displays a substantial interval of algebraic decay, as described by equation (10).

The fractions s_l and s_a, and the susceptibility-like quantities χ_l and χ_a were also sampled. The finite-size dependence of these quantities at criticality is shown in table 1. These quantities are well described by power laws as a function of the lattice size L for sufficiently large L. This is just as expected on the basis of finite-size scaling as expressed by equations (14), (18), (20) and (22). This behaviour is illustrated in figures 3–6.

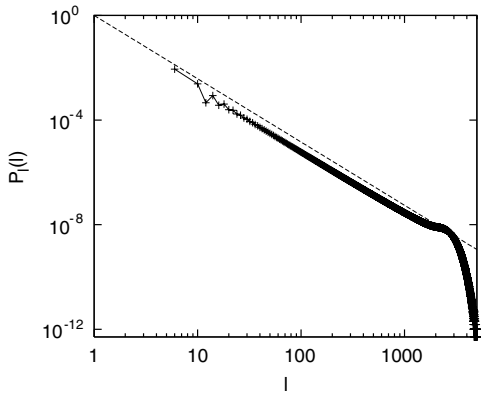

Figure 2. Distribution P_l of loops of length l on logarithmic scales, for the critical O(n) model with $n = 1.5$ and size $L = 128$. The dashed line shows a power law decay with exponent -2.42198318, which is the theoretical asymptotic value for the infinite system.

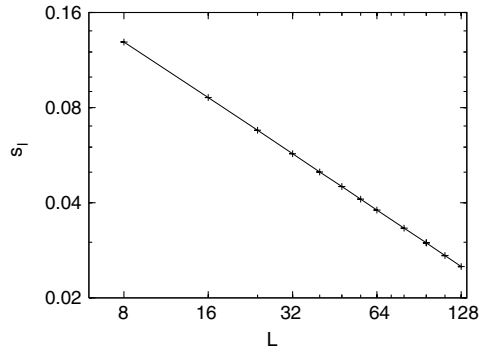

Figure 3. Fraction s_l of lattice edges covered by the largest loop, versus system size L for the critical O(n) model with $n = 1.5$, on logarithmic scales. The curve is added as a guide to the eye, and estimated error bars are smaller than the size of the symbols.

Using the nonlinear Levenberg–Marquardt least-squares algorithm, we fitted for the exponents and amplitudes according to the finite-size-scaling formulae including correction terms, as given in equations (15), (19). Thus we can numerically determine X_l, X_a, and thereby the fractal dimension d_l of the largest loop, and the fractal dimension d_a of interior of the largest loop. Comparing the residual χ^2 of the fits with the number of degrees of freedom, we find satisfactory fits including all system sizes $L \geqslant 8$. We obtain $X_l = 0.593(2)$ from the fit of $s_l(L)$ and $X_l = 0.595(2)$ from the fit of $\chi(L)$. These results are consistent with the theoretical value $X_l \approx 0.593\,513\,601$. The fit of $s_a(L)$ yields $X_a = 0.080(1)$. From the fit of $\chi_a(L)$, we obtain $2 - 2X_a = 1.84(1)$, or $X_a = 0.080(5)$. These results agree well with the theoretical prediction $X_a \approx 0.080\,108\,5234$.

In these fits, the correction-to-scaling exponent y_i was left free. The fits suggest that the exponent of the dominant correction to scaling does not assume the expected value $2 - X_{2l} = -0.438\,59$, but instead $y_i = -0.75 \pm 0.10$. On the other hand, we have also performed similar simulations of the O(1) model at the critical point. The fractions s_l and

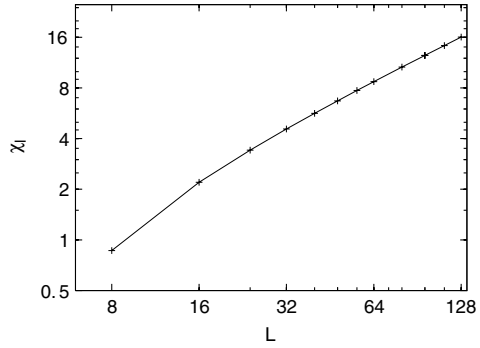

Figure 4. Susceptibility-like quantity χ_l versus system size L for the critical O(n) model with $n = 1.5$ on logarithmic scales. The curve is added as a guide to the eye, and estimated error bars are smaller than the size of the symbols.

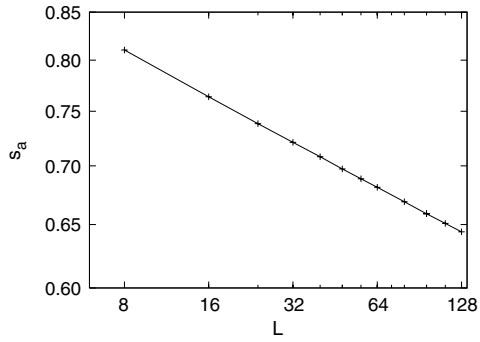

Figure 5. Fraction s_a of the number of dual lattice sites inside the largest loop, versus system size L for the critical O(n) model with $n = 1.5$, on logarithmic scales. The curve is added as a guide to the eye, and estimated error bars are smaller than the size of the symbols.

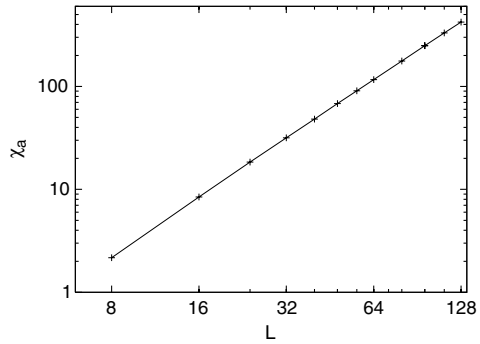

Figure 6. Susceptibility-like quantity χ_a versus system size L for the critical O(n) model with $n = 1.5$ on logarithmic scales. The curve is added as a guide to the eye, and estimated error bars are smaller than the size of the symbols.

s_a, and the susceptibility-like quantities χ_l, χ_a were sampled for several system sizes. The results are shown in table 2. Least-squares fit results agree well with the theoretical prediction, as listed in table 6. For the O(1) model, only the data for χ_l allowed a reasonably accurate estimate of the leading correction-to-scaling exponent. In this case, we find $y_i = -0.628(7)$,

Table 2. Numerical data for $s_l(L)$, $\chi_l(L)$, $s_a(L)$ and $\chi_a(L)$ for several system sizes L at the critical point of the O($n = 1$) model.

L	s_l		χ_l		s_a		χ_a	
8	0.091 26	(2)	0.435 32	(8)	0.883 55	(2)	1.1563	(6)
16	0.060 15	(2)	1.1859	(2)	0.850 90	(5)	4.580	(5)
24	0.046 78	(2)	1.8531	(3)	0.832 57	(7)	10.108	(16)
32	0.039 11	(2)	2.4658	(4)	0.819 87	(9)	17.682	(39)
40	0.034 05	(3)	3.0413	(6)	0.810 15	(12)	27.27	(8)
48	0.030 40	(3)	3.5901	(8)	0.802 34	(14)	38.73	(13)
56	0.027 54	(3)	4.1149	(12)	0.796 17	(15)	51.68	(19)
64	0.025 39	(4)	4.6235	(14)	0.790 38	(20)	66.98	(32)
80	0.022 14	(5)	5.5903	(24)	0.780 77	(27)	104.0	(7)
96	0.019 68	(5)	6.5121	(33)	0.773 84	(28)	145.3	(11)
112	0.017 81	(6)	7.4027	(42)	0.767 99	(35)	193.0	(18)
128	0.016 45	(6)	8.2442	(43)	0.762 13	(42)	253.2	(26)

Table 3. Numerical data for $s_l(L)$, $\chi_l(L)$, $s_a(L)$ and $\chi_a(L)$ for several system sizes L at the critical point of the O($n = \sqrt{2}$) model.

L	s_l		χ_l		s_a		χ_a	
8	0.121 86	(2)	0.7813	(1)	0.824 29	(3)	1.953	(1)
16	0.081 04	(2)	1.9989	(3)	0.780 04	(5)	7.651	(7)
24	0.063 61	(3)	3.1027	(5)	0.755 86	(8)	16.65	(2)
32	0.053 58	(3)	4.1362	(7)	0.7392	(1)	28.81	(5)
40	0.046 93	(4)	5.1183	(11)	0.7264	(1)	44.12	(9)
48	0.042 06	(4)	6.0630	(16)	0.7164	(2)	62.14	(18)
56	0.038 35	(5)	6.9786	(18)	0.7081	(2)	82.86	(22)
64	0.035 36	(4)	7.8623	(22)	0.7011	(2)	106.5	(3)
80	0.030 96	(5)	9.580	(4)	0.6890	(2)	162.4	(6)
96	0.027 69	(5)	11.222	(5)	0.6800	(3)	227.0	(12)
112	0.025 32	(6)	12.825	(7)	0.6716	(3)	304.4	(18)
128	0.023 38	(6)	14.370	(9)	0.6649	(4)	390.7	(25)

in a good agreement with the expected value $2 - X_{2l} = -0.625$. We thus have fixed y_i at this value in the other fits.

Furthermore, we performed similar simulations of the O(n) models with $n = \sqrt{2}$, $n = \sqrt{3}$ and $n = 2$ at their critical points as given in [2]. The fractions s_l and s_a, and the susceptibility-like quantities χ_l, χ_a were sampled for several system sizes. The results are shown in tables 3–5. Also these quantities appear to depend algebraically on the system size L, in agreement with the finite-size scaling equations (14), (18), (20) and (22).

Using a similar procedure as described above, we determined the exponents X_l and X_a. The results are summarized in table 6.

5. Discussion

The time-consuming character of simulations of loop models is, at least in part, due to the nonlocal character of the loops. We have reduced this problem by splitting the loop weight n in two parts, namely $n - 1$ and 1. Proper summation over both contributions is done by assigning colour variables to the loops; a sum on all colour variables is included in the partition sum.

Table 4. Numerical data for $s_l(L)$, $\chi_l(L)$, $s_a(L)$ and $\chi_a(L)$ for several system sizes L at the critical point of the O($n = \sqrt{3}$) model.

L	s_l		χ_l		s_a		χ_a	
8	0.151 97	(2)	1.1247	(2)	0.766 86	(3)	2.891	(1)
16	0.102 86	(2)	2.8312	(3)	0.714 34	(5)	11.150	(6)
24	0.081 69	(3)	4.4245	(7)	0.686 06	(6)	24.00	(2)
32	0.069 29	(4)	5.9453	(12)	0.666 77	(9)	41.16	(5)
40	0.061 11	(4)	7.4130	(17)	0.6522	(1)	62.44	(9)
48	0.055 00	(4)	8.8463	(23)	0.6408	(1)	87.21	(13)
56	0.050 35	(4)	10.241	(3)	0.6314	(1)	115.7	(2)
64	0.046 65	(4)	11.611	(4)	0.6233	(1)	148.0	(3)
80	0.041 12	(5)	14.272	(6)	0.6098	(2)	223.7	(6)
96	0.037 01	(4)	16.885	(7)	0.5993	(2)	311.0	(9)
112	0.033 87	(4)	19.407	(9)	0.5906	(2)	411.4	(12)
128	0.031 53	(5)	21.865	(11)	0.5824	(2)	531.2	(19)

Table 5. Numerical data for $s_l(L)$, $\chi_l(L)$, $s_a(L)$ and $\chi_a(L)$ of the critical O($n = 2$) model for several system sizes L.

L	s_l		χ_l		s_a		χ_a	
8	0.215 34	(3)	1.7038	(3)	0.664 65	(3)	5.082	(1)
16	0.152 73	(2)	4.4449	(7)	0.604 41	(3)	18.981	(6)
24	0.124 79	(2)	7.2121	(11)	0.572 83	(4)	39.965	(16)
32	0.108 12	(2)	9.9856	(17)	0.551 70	(4)	67.330	(29)
40	0.096 74	(2)	12.762	(2)	0.536 00	(5)	101.00	(5)
48	0.088 32	(2)	15.544	(3)	0.523 58	(5)	139.39	(7)
56	0.081 77	(3)	18.328	(4)	0.513 36	(6)	183.47	(11)
64	0.076 50	(2)	21.106	(4)	0.504 68	(5)	232.70	(14)
80	0.068 44	(3)	26.676	(7)	0.490 57	(7)	345.66	(30)
96	0.062 43	(2)	32.251	(9)	0.479 44	(6)	476.81	(37)
112	0.057 83	(3)	37.828	(11)	0.470 13	(7)	626.4	(5)
128	0.054 10	(3)	43.392	(13)	0.462 23	(7)	793.1	(7)
192	0.044 18	(3)	65.680	(26)	0.439 16	(10)	1620	(2)

Table 6. Results for the exponents X_l and X_a for five O(n) models, as obtained from least-squares fits as described in the text.

n	X_l from s_l		X_l theory	$2 - 2X_l$ from χ_l		X_a from s_a		X_a theory	$2 - 2X_a$ from χ_a	
1	0.625	(1)	5/8	0.73	(2)	0.0518	(3)	0.052 08	1.89	(1)
$\sqrt{2}$	0.599	(1)	3/5	0.796	(5)	0.075	(1)	3/40	1.86	(1)
1.5	0.595	(3)	0.5935	0.810	(4)	0.080	(1)	0.080 11	1.84	(1)
$\sqrt{3}$	0.571	(1)	0.5714	0.856	(1)	0.095	(1)	0.0952	1.81	(1)
2	0.4997	(3)	1/2	0.996	(5)	0.1249	(4)	1/8	1.747	(2)

The algorithm treats these colour variables as dynamical variables which are updated by the Monte Carlo process. The idea to use an additional colour variable for each loop was already used in a context unrelated to Monte Carlo methods, e.g. in [23]. An algorithm described by

Chayes and Machta for the simulation of the random-cluster model [24] uses the similar idea to assign colour variables to random clusters.

The presence of loops of weight 1 in a loop configuration then leads, at least locally, to a system that behaves precisely as an Ising configuration. Thus, the system may be locally updated by means of Metropolis-like Monte Carlo steps. Care should be taken to leave the loops of weight $n - 1$ unchanged, because it would violate the condition of detailed balance. The procedure given in section 3 satisfies this constraint.

The development of this colouring algorithm was motivated by the possibility of further exploring the physics of O(n) models. In the course of this work, we realized that it should be possible to construct an even more efficient algorithm of a 'cluster' nature, in analogy with the algorithms described by Swendsen and Wang [22] and by Wolff [26]. Algorithms of this type will be presented elsewhere [27]. The 'colouring' trick is only useful for $n > 1$. For $0 < n < 1$, the existing algorithm [18, 19] is, although relatively inefficient, still applicable.

For the interpretation of the simulation results, it is relevant that we are using periodic boundary conditions, and that the mapping between loop and Ising configurations imposes a condition of 'evenness' on the loop configurations: a path spanning the periodic boundaries must have an even number of intersections with a loop. Therefore, the statistical ensemble generated by the algorithm does not coincide with that of equation (4). The difference is related to the boundary conditions and is expected to modify the finite-size behaviour, but should vanish in the thermodynamic limit.

The present work is restricted to the 'even' loop configurations. It is, however, possible to simulate 'odd' loop configurations by introducing a 'seam' on the dual lattice, a vertical column of horizontal antiferromagnetic Ising bonds spanning the system. For these antiferromagnetic bonds, we use the rule that there is a loop segment if and only if the two associated dual spins are of the same sign. Horizontal and vertical seams can be introduced independently, as prescribed by the class of loop configurations that is to be sampled.

Acknowledgments

We wish to thank Professor B Nienhuis for several valuable discussions and suggestions. This work was supported by the NSFC project 10675021, and by the Lorentz Fund (Leiden University).

References

[1] Stanley H E 1968 *Phys. Rev. Lett.* **20** 589
[2] Nienhuis B 1982 *Phys. Rev. Lett.* **49** 1062
Nienhuis B 1984 *J. Stat. Phys.* **34** 731
[3] Kosterlitz J M and Thouless D J 1973 *J. Phys. C: Solid State Phys.* **5** L124
Kosterlitz J M and Thouless D J 1973 *J. Phys. C: Solid State Phys.* **6** 1181
[4] Domany E, Schick M and Swendsen R H 1984 *Phys. Rev. Lett.* **52** 1535
[5] Domany E, Mukamel D, Nienhuis B and Schwimmer A 1981 *Nucl. Phys.* B **190** 279
[6] Fisher M E 1967 *Phys., NY* **3** 25
[7] Wu F Y 1982 *Rev. Mod. Phys.* **54** 235
[8] Kasteleyn P W and Fortuin C M 1969 *J. Phys. Soc. Japan* **46** 11 (Suppl.)
Fortuin C M and Kasteleyn P W 1972 *Phys., Amsterdam* **57** 536
[9] Coniglio A and Peruggi F 1982 *J. Phys. A: Math. Gen.* **15** 1873
[10] Coniglio A 1989 *Phys. Rev. Lett.* **62** 3054
[11] Blöte H W J, Knops Y M M and Nienhuis B 1992 *Phys. Rev. Lett.* **68** 3440
[12] Deng Y, Blöte H W J and Nienhuis B 2004 *Phys. Rev.* E **69** 026123
[13] Janke W and Schakel A M J 2004 *Nucl. Phys.* B **700** 385

[14] Vanderzande C 1992 *J. Phys. A: Math. Gen.* **25** L75
[15] Nienhuis B 1987 *Phase Transitions and Critical Phenomena* vol 11 ed C Domb and J L Lebowitz (London: Academic)
[16] Saleur H and Duplantier B 1987 *Phys. Rev. Lett.* **58** 2325
[17] Duplantier B and Saleur H 1989 *Phys. Rev. Lett.* **63** 2536
[18] The existence of such an algorithm is already quoted by Karowski M, Thun H J, Helfrich W and Rys F S 1983 *J. Phys. A: Math. Gen.* **16** 4073
[19] Guo W-A and Blöte H W J 2001 unpublished
[20] Kadanoff L P 1978 *J. Phys. A: Math. Gen.* **11** 1399
[21] Nijs M P M den 1984 *J. Phys. A: Math. Gen.* **17** L295
[22] Sweeny M 1983 *Phys. Rev.* B **27** 4445
[23] Blöte H W J and Nienhuis B 1989 *J. Phys. A: Math. Gen.* **22** 1415
[24] Chayes L and Machta J 1998 *Physica* A **254** 477
[25] Swendsen R H and Wang J-S 1987 *Phys. Rev. Lett.* **58** 86
[26] Wolff U 1988 *Phys. Rev. Lett.* **60** 1461
[27] Deng Y, Guo W-A, Garoni T, Sokal A D and Blöte H W J 2007 *Phys. Rev. Lett.* (at press)